

# An auto-encoder bio medical signal transmission through custom convolutional neural network

Usha Maniraju, Thangamuthu Senthil Kumaran

Department of Computer Science and Engineering, ACS College of Engineering, Bangalore, India

## Article Info

### Article history:

Received May 16, 2023

Revised Sep 29, 2023

Accepted Oct 21, 2023

### Keywords:

Biomedical signals

Cloud

Compressive sensing

Internet of things

Proposed system convolutional neural network

## ABSTRACT

The transmission of biomedical signals in real-time is extremely difficult and necessitates the use of cloud and internet of things (IoT) infrastructure. Security is also an important consideration, however, to achieve this, a reconstruction method is developed where the entire signal is fed as an input, just the primary portion, the entire signal is taken then encoded, and then deliver to the destination. It is unlocked using a reconstruction technique without any signal attenuation. The key difficulty is how to manage the sensor network once the input is prepared for transmission. This has problems with extremely high network energy consumption and accurate data collection. The accuracy of data reconstruction through is improved by compressive sensing. The lifespan of the network as a whole could be extended, in this study; the proposed proposed system convolutional neural network (PS-CNN) is an integrated model that combines feature selection and auto-encoder. In order to produce the most useful features for particular tasks, our algorithm can eventually separate the appropriate task units from the irrelevant tasks.

*This is an open access article under the [CC BY-SA](https://creativecommons.org/licenses/by-sa/4.0/) license.*



## Corresponding Author:

Usha Maniraju

Department of Computer Science and Engineering, ACS College of Engineering

Bangalore, India

Email: usharaj.@gmail.com

## 1. INTRODUCTION

WSNs, which stands for “wireless-sensor-networks,” is a type of network that is composed of sensor nodes (SNs), and each SN is responsible for data processing, sensing, and communication. WSNs can be used for a wide variety of applications, including environmental monitoring, agriculture, military surveillance, police international boundaries, and the rising need for machine health monitoring. WSNs already make up a significant portion of the internet of things (IoT) infrastructure necessary for smart living [1]. At the physical layer, the IoT provided a powerful data interchange for all of the connected items. The IoT can be recognized by its characteristic feature, which is the connectivity of data-sensing terminals such as global positioning system (GPS), radio frequency identification (RFID), sensor network (SNs), and ultra-red identifiers in order to carry out communication and data exchange for the predefined protocol. Tracking, intelligent object identification, object management, and location are all common applications of the IoT. It is frequently organized into three layers, with the transmission layer, the sensor layer, and the application layer being the most common configurations.

The transmission layer is responsible for obtaining reliable data transmission (DT) between the application layer and the sensing layer in order to cut down on packet loss and network delay while simultaneously improving accuracy and the rate at which data is collected. In recent years, a number of initiatives that aimed to implement an energy-saving strategy for the data transmission of WSNs are

successfully completed. In order to extend the lifespan of the sensor node (SN), it is essential that the amount of energy that it consumes while transmitting data be maintained to an absolute minimum. Both the compression and the aggregation of data are common approaches that are taken in the pursuit of this aim. The transmission of redundant data-by-data processing is cut down significantly by aggregating the data that is received from several sensors. The primary goal of data aggregation is to identify instances of redundancy in the data that is created by neighboring sensors [2]. In view of transmitting the raw sensing data, the fundamental objective of data aggregation is to aggregate the output of several sensors while maintaining a predetermined amount of redundancy. Every single sensor node (SN) that is a part of this aggregate sends out data packets with the exact same dimensions and counts at different times. The way in which the network predicts the value known as the partial rate for the subsequent mid-node in the aggregation tree is affected by each data packet that is transmitted. Even when the amount of data that is supplied is decreased as a concern of data aggregation, there is still a possibility that vital data may be lost due to the calculation of duplicated samples. In addition to this, its anti-noise ability is quite subpar, and a data transmission network with higher quality is required. The spatial-temporal correlation has a significant influence on aggregate outcomes at the same time as it does. Encrypting data with the encoding method is another approach tackled. The S-LZW (Lempel-Ziv-Welch) compression method is one method that can be used to reduce the size of the dictionary [3]. The static Huffman approach makes use of a specified probability table in order to achieve the benefits of Huffman compression [4]. The adaptive Huffman method uses the branches, leaves, and nodes of the tree model to represent the information that is being conveyed. Finishes writing up the manuscript on the Z-order-based data compression approach [5]. However, because repeating data is typically the subject of coding, compression is frequently confined to levels that are very close to lossless compression. This is because lossless compression is difficult to achieve.

The compressive sensing (CS) techniques serve as a novel tool for signal processing and acquisition, which allows for the analysis of data in WSNs [6]. The findings demonstrate that data acquired largely via CS-based techniques can fully utilize benefits offered by spatial networks, lower the amount of energy consumed by networks, make data compression simpler, and prevent concerns relating to energy holes [7]. In any event, the CS-based data collection method in WSNs is focused on the environment of a dependable network in which there is a lack of packets on the network links. This is the case because the method was developed for this environment. Loss of packets is common in WSNs that simulate the real world.

In addition, one may deduce from the findings that the number of data packets that are lost has an effect on the efficiency of the CS-based data-gathering methods. For example, there is less loss of packet data, and the techniques of data gathering cannot guarantee the efficacy of network recovery data. In spite of the fact that a few solutions have been suggested for sparse random projection in order to decrease the consequences of packet loss, no actual design has been offered for the basis of the sparse expression. As a result, it is hard to validate the universality of these solutions.

In order to solve the issue described in the previous paragraph, our proposed system convolutional neural network (PS-CNN) is a proposed solution that combines the auto-encoder and feature selection processes. On the learned hidden layer, feature selection is utilized in an automated manner to separate discriminative features from irrelevant ones. This keeps the layer organized. Immediate feedback from task-relevant hidden units can be used to enhance the encoding layer and raise the discriminability of the chosen hidden units. After that, the multi-hop function between the SNs, which our proposed method employs to derive, may be applied to figure out the proportional relationship between SNs. An observation with a lower correlation is made based on the reconstruction approach in order to cut down on data packet loss on the IoT and increase the accuracy of data reconstruction for base stations. This helps ensure that the data is reconstructed correctly. In order to acknowledge the process that is responsible for the data aggregation technique, which is subsequently employed to strengthen the dependability of data transmission across clusters. The contribution of this research can be summed up using the points that are presented below. In this article, we look at several lossy compression strategies, such as those based on temporal and spatial dynamic signals that are based on a range of different techniques. The next topic that will be covered is compressive sensing, which is a set of techniques that make use of signal correlation in both time and space. The sampling techniques that are based on compressive sensing make use of the correlation structure of the signal. This structure is advantageous to the selection nodes, which in turn improves the performance of the reconstruction.

The CNN-PS is the center of the work in the integrated architecture. It delivers complementary performance in terms of feature selection and auto-encoder, and it is the primary component of the work. The framework chooses to distinguish higher-level characteristics in order to strengthen the discriminability of the units that have been selected. Our proposed method can be improved in a variety of contexts, such as clustering, by transferring the feature selection criteria to the hidden layer. These criteria include the Laplacian score and the Fisher Score. A foundation for stacked networks is provided by the PS-CNN that is developed. In the end, we carry out a large number of experiments to evaluate the efficiency of our method in

comparison to that of other algorithms in terms of the reconstruction error, the packet arrival rate, the amount of time the network is active, and the amount of energy it consumes. Because of this, the efficiency and validity of our suggested method have been demonstrated.

In the second part of this investigation, a summary of the previous research on compressive sensing and energy consumption in wireless sensor networks is presented. In section 3, we present the CNN-PS algorithm, which merges the feature selection and auto-encoder into a single process. The performance of our investigation is evaluated in section 4 with regard to energy consumption, the rate at which packets arrive, and reconstruction errors, and section 5 concludes at the end. When building mobile multimedia and WSN healthcare applications, one of the most significant factors to take into consideration now is the amount of energy that is consumed. A variety of strategies is implemented in WSN in order to cut down on the amount of energy that is consumed.

The first description of the wake-up radio appeared in [8]. This radio automates the sensor nodes (SN) and reduces response latency, hence controlling and minimizing the energy consumption of WSN. This approach is used for enhanced energy consumption sensors in a two-tier WSN for video/camera surveillance applications since its infrared SNs have a lower energy consumption. In contrast to [9], which demonstrated the heterogeneous multitier wireless prototype of a multimedia sensor network (WMSN) using low-power hardware technologies, [9] also listed a number of references in support of this claim. This prototype employs a network architecture that supports three unique modes of operation; these modes are referred to as shutdown, sleep, and wake-up, respectively.

## 2. RELATED WORK

Compressive sensing, also known as CS, has garnered a lot of interest in a wide variety of applications, including video processing [10], machine-type communications [11], physical layer operations [12], cognitive radio networks [13], imaging [14], and radar signal processing [15]. Channel estimate in wireless networks [12] and channel estimation in power communication cables [16] are two examples of other uses. In early works relating to computer science, the methodologies and broad applications of computer science are presented. The applications of computer science in WSNs for distributed compression, source localization, and compressed data collection have been investigated as part of the larger topic known as “CS for networks and communications”. The use of CS for communication networks is also presented in [17], with an emphasis on receiving input from various layers once application, physical, and network actions have been finished. There are a number of topics that are unique to WSNs, such as the routing of compressed data in a centralized environment and collection of compressed data that investigates geographical and temporal sparsity [18]. While the authors of [18] focused on considerations that must be made while using the CS for wireless communication’s symbol detection, interference cancellation, support identification, and channel estimation, as well as relevant to a variety of application scenarios, Huang *et al.* [18] also emphasized the importance of taking into account factors that are relevant to a number of different application scenarios. A few of the operations have been presented in [19] because simultaneous sparse signal recovery utilizing source localization and multiple measurement vectors (MMVs) can be applied to WSNs.

In addition, Razzaque *et al.* [20] has provided a comprehensive comparison of the methodologies of data centric system (DCS), adaptive sampling (AS), transform coding (TC), and predictive coding (PC). The primary study analyzed data from three separate datasets, which included temperature data, data on CO2 emissions, and seismic signal data. The total findings indicate that the CS achieves the greatest amount of energy savings by a factor of 79.4%, in contrast to the AS and TC, which achieved savings of 34% and 62.43%, respectively. While [21] compared the labelling and segmentation approaches [22] that have been taken into consideration for the IEEE 1451 standard, based on the amount of time it took to calculate and the quality of the reconstruction, [22] carried out a comparison of the methodologies. The findings indicate that the CS has a nature that is exceedingly complicated and that it outperforms conventional labelling and segmentation methods, which are primarily predicated on data reconstruction and noise robustness, by a substantial margin. On the other hand, [23] computes the ideal placement based on event data, which has the potential to effectively minimize network balance load and transmission distance. The path of optimal movement for the sink node is also designed in order to increase the efficiency of movement. Additionally, data inside the cluster are integrated in order to limit the amount of redundant information that is transmitted. Because of this, the structure of the network routing is preserved in an effective manner, and the dependability of the data transmission is established. Whereas [24] portrayed the large strength of a big data and the IoT-based application, system [25] focuses on the internet of things (internet of things). They used cloud-to-end fusion as the system architecture for the most essential health application. This system is made up of multiple levels, some of which are for transportation, others for public health, and others for

cloud-based perception. One of the most significant challenges in transitioning between these layers is the expenditure of energy, in particular in wireless communication over short distances.

### 3. PROPOSED METHODOLOGY

In this section, the bio-medical signals are modeled, which are evaluated towards an optimized Auto-encoder algorithm, which is used for performance evaluation. Here the techniques are verified across the signals that authorize the generation of signals for a time-independent spatial field to tune the feature correlation. This is essential for managing the correlation degree in variation with time and space that is accessible to provide an effect on the performance of a selection of compression.

#### 3.1. Fine-tuning the spatial field for feature correlation

Here the techniques are verified across the signals that authorize the generation of signals for a time-independent spatial field to tune the feature correlation. This is essential for managing the correlation degree in variation with time and space that is accessible to provide an effect on the performance of a selection of compression. The target application provides an example of the sensor field at appropriate intervals. The time slot is depicted as  $x$  fixed to the value as  $\Delta x$ . The spatial and temporal domains are depicted as  $ST = \{x_k = k\Delta | x = 0, 1, 2, \dots\}$  and  $\psi = [-u_i, u_i] \times [-v_i, v_i]$ . In space, the point is focused as  $x = (u, v) \in \psi$ .  $a(x, y): \psi \times \omega \rightarrow \mu$  to symbolize this signal which is generated through the constant in space and time along with variance denoted as  $\sigma_u^2 = 1$ , where the mean is denoted as  $m_u = 0$  which is further tuned through the correlation. In the spatiotemporal environment modeling, the tuning correlation function is shown in separate time and space components.

$$\omega_{u,v}(x_1, y_1, x_2, y_2) = \omega_U(x_1, x_2) \omega_V(y_1, y_2) \quad (1)$$

Here  $x_1$  and  $x_2$  are two points shown in, the parallel time constants as shown as  $y_1$  and  $y_2$ ,  $w_u(\cdot)$  and  $w_v(\cdot)$  depicts the spatial and temporal signals. The stationary signal is allotted the value of function  $h = \|x_2 - x_1\|_2$  and  $\Delta y = y_2 - y_1$ . The signal is generated for an appropriate function is used. Then  $\omega_U(h)$  denotes the Gaussian function.

$$\omega_U(h) = \exp\left\{-\frac{h^2}{\varphi c^2}\right\} \quad (2)$$

In (2)  $h$  depicts the scaling factor, very dependent on the field size and  $\varphi$  indicates the parameter used for controlling the spatial correlation.

##### 3.1.1. Sensor node transmission routing

A set of sensor nodes  $\eta_0$  with  $|\eta_0| = \rho$  is uniformly classified randomly through the area with  $\psi$  with  $u_i = v_i = 50m$ . The transmission mode is in the range  $\psi$ , by assuming a model for sensors that can transmit within these nodes are situated that locate the distance in a shorter range that is equal to  $\mu$ . Here  $\mu = 2u_i \frac{\sqrt{5}}{\sqrt{\eta_0}}$  enables us to confirm the structure that is interrelated through the high-probability model deployment. The mobile sink is located in the middle of WSN. While routing each sensor is allocated the next hop through the node within the range that depicts huge development in the direction of the mobile sink.

Here the delay function for time-slot  $v$  is shown as the time slot for collecting data, the sensors here are responsible for process scheduling to retain the quantity of the example nodes' time per each slot  $v$ . In each time slot, the mobile sink collects compression of data from sensors. This is designed by the reading aggregation that is allotted for a specific amount of time window for  $v$  slots through various payload packets.

##### 3.1.2. Weighted clustering algorithm

The weighted clustering algorithm is used with the help of a deterministic source, this algorithm results in a sensor that is preliminary analysis shown for the number of clusters  $\eta_c$  that is focused on the segmentation of the area of WSN. A cluster head is picked for each cluster set so that  $\varpi$  minimizes the distance between other clusters. The compression technique expedites the energy consumed the total energy cost is associated with the compression method that functions along with the sensor nodes which involves the computation cost. The data delivered, and the energy consumption by the mobile sink is achieved through more than one routing path known as data delivery. The packets are transmitted from the mobile sink to the sensor nodes via a multi-hop procedure.

### 3.2. Compressive sampling techniques

In the compressed sensing mechanism, the compression selects each data and the node selects to transmit the sensing across the corresponding reading. In this section the random sampling method gives the value of  $\mu(y)$ , the main goal here is to share the workload between the nodes. Whereas the sampling of sensors results in an advantage based on the construction of signal at the mobile sink. However, the sampling techniques are evaluated in this section.

#### 3.2.1. Compressive sensing-based node selection

The nodes here are transmitted on an average basis for the time slot  $y = 0, 1, 2, \dots$ , to the mobile sink. A simple disseminated approach to obtain a transmission probability of  $x_{yu} = \beta x_{yu}$ . Every single node is independently selected irrespective of the sample to be transmitted to the mobile sink for  $p_{yi}$ . This is specifically responsible for keeping the payload packet transmitted to the mobile sink through multihop-routing. The user  $k \in \{1, \dots, \beta\}$  transmits at the same-time slot  $v$ .  $\mu(y)$  in the  $k$  th column.

#### 3.2.2. Compressive sensing sampling for predictive node selection

The node selection is responsible for sampling that integrates the data  $n$  at each round. Both these methods operate with data collection for different time-slots  $\tau$ . Compressive sensing-based random sampling is necessary for the evaluation of various techniques by considering the mobile sink spread across WSN nodes by multi-hop routing. At each time slot  $y \in \{1, 2, \dots, \tau\}$  and these nodes are selected by two methods. The nodes selected for  $v$  time-slot are explained in detail by the monitored approach.

Henceforth,  $\mu(y)$  consists of only one column where  $k \in \{1, \dots, \eta\}$  for the time slot  $y \in \{1, \dots, v\}$ , the schedule here is monitored based on node  $k$  for transmission across the time slot. The efficiency is enhanced here by the data aggregation approach, which is sampled for transmission across random sampling. For each time slot, the sensor is sampled through the signal for the time slot allotted by a monitoring schedule. In the last time slot  $\eta$  the sensor here combines the reading to store it for single and multiple payload packets for transmission to the mobile sink for processing. The mobile sink collects the packet received and transmitted it to the sampling matrix.  $\mu(y)$  Determines its nodes with corresponding time-slots that incorporate to get  $g(y)$  at the mobile sink for all the time-slots  $\in \{1, \dots, \eta\}$ . this iteration is repeated for the entire set. The two heuristic processes for evaluation of monitoring procedure. The spatial correlation is based on the sensors for these algorithms. An  $n$  loads huge improvisation for reconstruction in the mobile sink.

#### 3.2.3. Predictive node selection for feature correlation

The first-round collection of the time slots for  $\{1, \dots, \eta\}$  considered for  $\eta = \beta/\beta$ . consider  $E$  and  $F$  for Gaussian random variables, here  $F \sim \beta(l_g, \beta_g)$  and  $E \sim \beta(l_u, \beta_u)$  here  $l$  and  $\beta$  determine mean and standard deviation. The variance  $F$  and  $E$  are equivalent to  $\beta_b^2(1 - \rho_{ab}^2) = \beta_b^2 - \left(\frac{\beta_{uv}}{\beta_u}\right)^2$ ,  $\forall u$  here  $\rho_{uv} = \beta_{uv}/\beta_u\beta_v$  depicted as the correlation between  $F$  and  $E$  the  $\beta_{uv} = \mathcal{E}[(E - l_u)(F - l_b)]$ . Here in  $\beta$  nodes for each  $k \in \beta$ , to evaluate the variance  $l_y$  for all sensors.

$$l_y = \sum_{k \in P} \beta_a^2 (1 - \omega_{ab}^2) = \sum_{k \in P} \beta_a^2 - \sum_{k \in P} \frac{\beta_{ab}^2}{\beta_b^2} \quad (3)$$

Here, the  $j^*$  is the smallest node with  $l_y$  that is shown as,

$$j^* = \underset{j \in P}{\operatorname{argmin}} \left( \sum_{k \in P} \beta_a^2 - \sum_{k \in P} \frac{\beta_{ab}^2}{\beta_b^2} \right) \quad (4)$$

Here the second one is followed by the first sum that is independent of  $y - th$  index. The metric is used as  $l_y$ .

$$l_y = \left( \sum_{k \in P} \frac{\beta_{ab}^2}{\beta_b^2} \right) \quad (5)$$

Here we denote the  $l_y$  is relevant to the correlation for the given value sampled for sensor and readings. to determine how this node is represented across the correlation of the pertaining value for  $l_y$  to depict different nodes in the sensor  $\beta$ .

The main challenge is to deliberate the aggregation of  $\eta$  selection consisting of  $\mu$  nodes. here each set is responsible to relate the slot time with the collection of rounds for sampling the time slot. To sort the sensors for correlating-DNS in  $P$  decreasing order. Hence we choose the sensors  $\eta$  with a high metric in this set to allow the time slots  $\{1, \dots, \mathcal{D}\}$  this follows the relevant method. This step is iterated until all the nodes are allotted. Here every single node samples the respective time slot.

$\mathcal{D} = \text{int}(\mu/\beta)$  This is serialized by the  $\mu/\beta$  and  $\text{int}$  integers. Here this schedule is accomplished through the previous iteration mechanism, which is multiplied by  $\text{int}$  number of times for data technologies. Here  $\mu/\beta$  is not this integer value, to sample some nodes twice for the  $\mu/\beta$  slots to assure these sampling nodes are depicted as. The nodes here the samples are reconstructed that shows the consumption of energy.

### 3.2.4. Optimization for predictive node selection based on feature correlation

The problem selection of  $\beta$  sensors for  $\mu$  nodes, for  $\mathcal{D} = 1$  the single-slot for the time-round is used for data collection. Here initialization of the nodes that are processed with  $v_1 = N_0$  and  $v_2$  is the empty set. The main aim here is to select the  $\mu$  nodes from  $v_1$  this leads to a small-reconstructed error for sensors not selected. Table 1 shows the node selection predictive correlation algorithm.

Table 1. Node selection predictive correlation algorithm

Step 1	Assume $v_2^y(k), y \in 1, \dots, \mathcal{D}$ for $\mathcal{D} + 1$ set and $k \in \{1, \dots, \beta\}$ for $k - \text{th}$ step of the iteration
Step 2	Consider $v_1(k)$ to select the nodes from $\mathcal{D}$
Step 3	Assign each node to the set $v_2^y(k)$ for $y \in \{1, \dots, \mathcal{T}\}$ .
Step 4	These nodes are discarded from $v_1(k)$
Step 5	If $k = \beta$ , else return to step 1

Here the  $\mathcal{D}$  sensors for each level are allotted to  $\mathcal{D}$  as the disjoint sets  $v_2^y(k)$ . To choose the best nodes for  $\mathcal{D}$  selections and halt whenever the given nodes are allotted the selection of  $\beta$  nodes. They are used for the metric that is based on (7) for each node selected that is removed from  $v_1$ , to determine the amount determine the statistics for the nodes left. The  $\mathcal{D}$  gives the algorithm of extended for node selection deterministic correlation algorithm that requires few nodes to resample the slots to rotate them and accommodate the energy consumption.

### 3.3. Optimized feature selection based on convolutional neural network (CNN) algorithm

A CNN-based algorithm is used for combining feature selection and auto-encoder, the feature selection process selects prominent data as the auto-encoder process compresses the data through a single algorithm. The feature selection of the hidden layer data. By considering  $F \in \delta^{s \times b}$  the training data for  $s$  direction for the virtual descriptor and the sample data depicted as  $b$ .

$$\min_{g_1, \theta_2, T_1, T_2, Z} \frac{1}{2} \|K - S(b(K))\|_b^2 + \frac{1}{2} \mu \vartheta(Z, b(K)) \quad (6)$$

Here  $b(K)$  and  $S(b(K))$  are shown as  $\sigma(\mathcal{W}_1 K + J_1)$  and  $\sigma(\mathcal{W}_2 b(K) + J_2)$  here  $J_1$  and  $J_2$  is the repeated column. The standard format for the prominent choice is depicted as  $\vartheta(Z, b(K))$  along with the matrix consisting of trained feature selection for data performance of  $b(K)$  represented as the hidden unit. Implicitly for  $O_a$   $\text{th}$  vector the column is depicted as shown as  $O_a \in \mathfrak{R}^z$ .

$$O_a = [\underbrace{0, \dots, 0}_{b-1}, 1, \underbrace{0, \dots, 0}_{c-b}]' \quad (7)$$

Here the hidden units are represented as  $c$  and the column vector as  $b$  this picks the unique feature of  $j \in \mathfrak{R}^m$ . The feature selection procedure results in the original feature as  $b(K)$  to discover the given matrix  $Z$  to select the set  $J = Z' b(K)$  that is optimized further for  $\vartheta(Z, b(K))$ .

The feature selection is divided into three categories such as supervised, semi-supervised, and unsupervised algorithms. The main aim of the supervised model that can conserve the data for feature selection using the fisher score [25], and the unsupervised content to preserve the structure of intrinsic data such as the laplacian score. This aims in dealing with various cases such as  $\vartheta(Z, b(K))$  in a generic way. The feature selection is introduced as:

$$\vartheta(Z, b(K)) = \frac{Q(Z'b(K)H_i b'(K)Z)}{Q(Z'b(K)H_l b'(K)Z)} \quad (8)$$

This shows a generic graph framework for feature selection. Several ways of constructing weight matrices such as  $H_i$  and  $H_l$  result in several features such as semi-supervised, supervised, and unsupervised selection algorithms. The main aim here is the feature selection of pursuing this with minimality by resolving this problem of optimization.

$$Z = \arg \min_Z \frac{Q(Z'b(K)H_i b'(K)Z)}{Q(Z'b(K)H_l b'(K)Z)} \quad (9)$$

The direct problem here is to solve the task of trace ratio for inaccessible solutions for the problem. This deals with the trace-ratio problem, the equivalent trace difference problem obtains a way to solve the issue of obtaining a solution of a global optimum. Assume the criteria score for subset level  $\vartheta(Z, b(K))$  substituting in (10) that reaches the global minimum  $\psi^*$  for;

$$\psi^* = \arg \min \frac{Q(Z'b(K)H_i b'(K)Z)}{Q(Z'b(K)H_l b'(K)Z)} \quad (10)$$

To describe the  $\psi$  function while treating the constant as;

$$\mu(\psi^*) = \arg \min_Z Q(Z'b(K)(H_i - \psi H_l)b'(K)Z) \quad (11)$$

To find the global optimum for  $\psi$  is transformed into the equation root,  $\mu(\psi^*) = 0$  to solve the issue of trace difference. Here  $\mu(\psi)$  to monotonically maximize the function. To represent the above problem for trace-difference in hidden layers of the auto-encoder function in the end formulating the final function as:

$$\min_{g_1, g_2, T_1, T_2, Z, \psi} \sigma = \frac{1}{2} \|Z - \zeta(b(K))\|_2^2 B + \frac{1}{2} \psi Q(Z'b(K)(H_i - \psi H_l)b'(K)Z) \quad (12)$$

In (12)  $\psi$  which is defined as the parameter for feature selection by incorporating auto-encoder term, which is optimized by the score of trace-ratio  $K$  is distinguished to solve the problem of trace-ratio optimization.

### 3.3.1. Non-linearity based optimization

The solution to the problem obtained by (12) is complex in solving the non-linearity constraint of the auto-encoder, whereas the alternate solution for optimization is used simultaneously to update the parameters of the auto-encoder.  $g_1, g_2, T_1, T_2$  and the variable feature selection for  $Z$  and  $\psi$ . To solve the problem of optimization for two sub-problems like that as feature-selection score and optimization of auto-encoder.

### 3.3.2. Feature selection-based learning

The parameter fixed for optimization of the feature selection score  $\psi$  and the feature selection of the  $K$ th matrix is the primitive technique of trace-ratio. The trace difference equation is shown in (13). Here  $Z_y$  is the optimal result in  $y$ -th optimization, hence  $\psi_y$  is computed as given in (14).

$$Z = \arg \min_Z Q((Z'b(K)(H_i - \psi H_l)b'(K)Z)) \quad (13)$$

$$\psi_y = \frac{Q(Z'_y b(K)H_i b'(K)Z_y)}{Q(Z'_y b(K)H_l b'(K)Z_y)} \quad (14)$$

Henceforth,  $\mu(\psi_y)$  is given in (15);

$$\mu(\psi_y) = Q(Z'_{y+1} b(K)(H_i - \omega_y H_l)b'(K)Z_{y+1}) \quad (15)$$

Whereas  $Z_{y+1}$  is computed by a rank score of each feature depicted. Table 2 displays the Algorithm 2. Then  $\mu(\psi) = 0$  in the equation's root to find the optimal criteria for feature selection that serves as the function to solve the parallel procedure of auto-encoder.

Table 2. Algorithm

Input	$b(K), H_l, H_i$
Step 1	Initialize: $Z = K, K \in \hat{\Gamma}^m$ and $\psi$ substituted in (21), $\epsilon = 10^{-9}$ $Max\_Itr = 10^3$ and $Itr = 0$
Step 2	While $Itr < Max\_Itr$ do not unite
Step 3	Compute the feature score of $jth$ value in (14)
Step 4	Ranking the feature selection score in ascending order
Step 5	Select the leading features of $m$ to update $Z \in \hat{\Gamma}^m$
Step 6	Compute $\psi$ by (14)
Step 7	Check the conditions that unite: $\ \psi_o - \psi\  < \epsilon$
Step 8	end
Output	$Z$ is the feature matrix and $\psi$ is the global optimum

### 3.3.3. Gradient function-based learning on auto-encoder

With (12) the different parameters considered are  $g_1, g_2, T_1, T_2$  using the stochastic-sub-gradient-descent method, here  $Z$  and  $\psi$  have a fixed value. The main gradient function  $H$  with the parameters evaluated as:

$$\begin{aligned} \frac{dH}{dT_2} &= \left( K - \zeta(b(K)) \right) \odot \frac{d\zeta(b(K))}{dT_2} b'(K), \\ \frac{dH}{du_2} &= \left( K - \zeta(b(K)) \right) \odot \frac{d\zeta(b(K))}{dT_2} = H_2, \\ \frac{dH}{dT_1} &= \left( T_2' H_2 + \omega Z Z' b(K) (H_l - \psi H_i) \right) \odot \frac{db(K)}{dT_2} K', \\ \frac{dH}{du_1} &= \left( T_2' H_2 + \omega Z Z' b(K) (H_l - \psi H_i) \right) \odot \frac{db(K)}{dT_2}. \end{aligned} \quad (16)$$

Here the  $g_1, g_2, T_1, T_2$  value is updated as gradient descent algorithm stated as:

$$\begin{aligned} T_1 &= T_1 - \varphi \frac{dH}{dT_1}, \quad u_1 = u_1 - \varphi \frac{dH}{du_1}, \\ T_2 &= T_2 - \varphi \frac{dH}{dT_2}, \quad u_2 = u_2 - \varphi \frac{dH}{du_2}, \end{aligned} \quad (17)$$

Here  $\varphi$  is defined as the learning rate,  $\frac{dH}{dT_1}$  and  $\frac{dH}{dT_2}$  are the column means for  $\frac{dH}{du_1}$  and  $\frac{dH}{du_2}$ . To sum up these issues this is upgraded simultaneously. Table 3 displays the Algorithm 3. In Algorithm 3 the optimization of the parameters is explained, wherein  $m < s$  denotes the number of features,  $\psi$  is the parameter considered,  $K$  is the learning data.

Table 3. Algorithm

Input	$K, \psi, m < s$ and $layer\_size$
Step 1	Initialization: $Max\_Itr_{Itr} = 50, Itr = 0, exp = 10^{-7}$
Step 2	While $Itr \leq Max\_Itr_{Itr}$ not unite do
Step 3	Upgrade $K$ and $\psi$ with (13), others kept constant
Step 4	$K$ is fixed and updated by (17) and $g_1, g_2, T_1, T_2$
Step 5	Check the condition that unites $\ H_n - H_o\ _\infty < \epsilon$
Step 6	End The new feature is shown as $U_{ts} = Z' \sigma(T_1 K_{ts} + U_1)$
Output	$Z, g_1, g_2, T_1, T_2 (U = Z' \sigma(T_2 K + U_1))$ Is the input of this algorithm, which forms the structure of the stack

## 4. RESULT AND ANALYSIS

In this section, the results are simulated using MATLAB, and the outcomes of the simulations demonstrate the viability and efficiency of our proposed PS-CNN. The related configurations are also covered in this section. The  $200 \times 200$  m square under surveillance has 280 densely placed SNs (sensor



nodes). The energy is 10J for each SN (sensor node). The sink's node is placed outside the area under observation. Data collection settings are  $W_1=0.5, 0.1$ , and  $0.4$ ;  $W_2=0.9, 0.5$ , and  $0.9$ ; the range of intervals is  $R=10$  m; and time is  $T=900$  s. After that, the proposed algorithm on the MIMIC-II [26] dataset to assess its robustness and generalizability.

The comparison of our proposed PS-CNN method with the current MIC-CSDG technique based on reconstruction error (RE) with various parameters is shown in Figures 1-3. Based on Figure 1, our PS-CNN method's improvement demonstrates the value of network running time whereas a competing approach is less clear when compared to our algorithm. In any case, when the amount of time a network may run increases, the existing algorithms demonstrate development. Our technique greatly outperformed the existing algorithm when the network was running for 800 s. As we can see in Figure 2, the performances for the existing method are developed when the network running time is close to 850 s. The performance of error is less effective than our proposed algorithm at the beginning of network running time. As we can see, while MIC-CSDG shows very rapid improvement and network operating time increases, our algorithm's performance is consistent. The parameters for Figure 2 are  $W_1=0.4$  and  $W_2=0.9$ . In contrast to the existing approach, our algorithm's performance also holds steady. The primary difference between our approach and the existing algorithm is that our algorithm maximizes. Furthermore, the issue of poor judgment at the sink node is diminished.

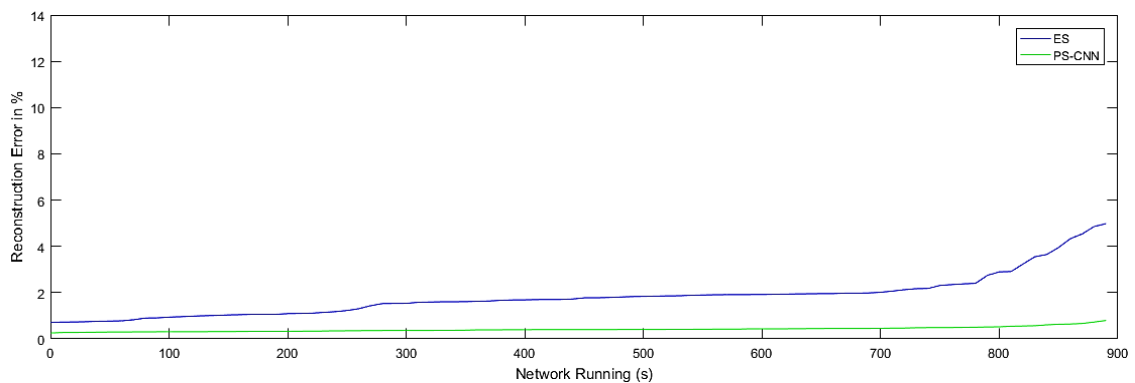


Figure 1. Comparison of RE with the existing algorithm at different parameters are  $W_1=0.5$  and  $W_2=0.9$

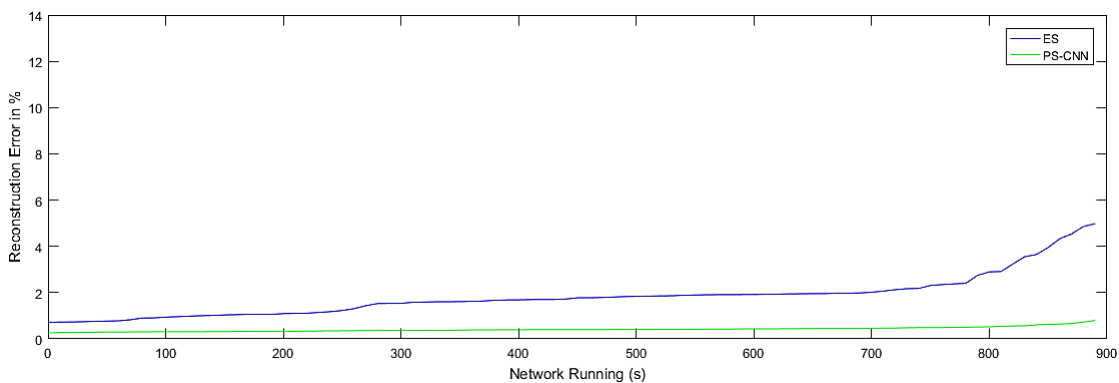


Figure 2. Comparison of RE with the existing algorithm at different parameters are  $W_1=0.1$  and  $W_2=0.5$

The packet loss is dealt with using the CNN-based optimized BCAE method. Figures 4 to 6 show the comparison of packet arrival rate (PAR) for various parameters. For simulations, 280 SNs are taken into account, and each SN sends out 50 messages. We compare the existing technique with CNN-PS using different  $p$ -values. Calculating the packets received at the sink node allows for the simulation results in Figures 4 to 6. Our proposed CNN-PS method satisfies the  $p^*$  criteria based on simulation results. For  $p^*=1$ , the PAR can be quite close to the theoretical UB (Upper Bound).

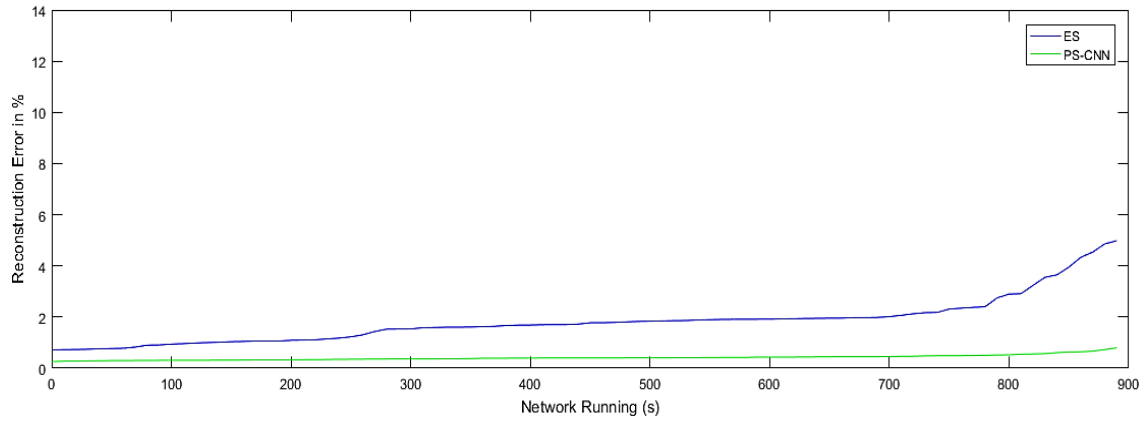


Figure 3. Comparison of RE with the existing algorithm at different parameters are  $W_1=0.4$  and  $W_2=0.9$

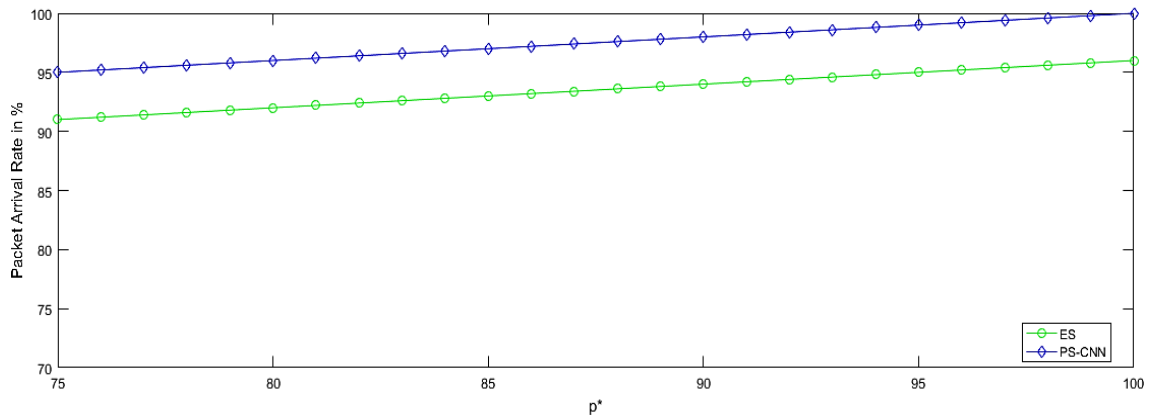


Figure 4. Comparison of PAR with the existing algorithm at different parameters are  $W_1=0.5$  and  $W_2=0.9$

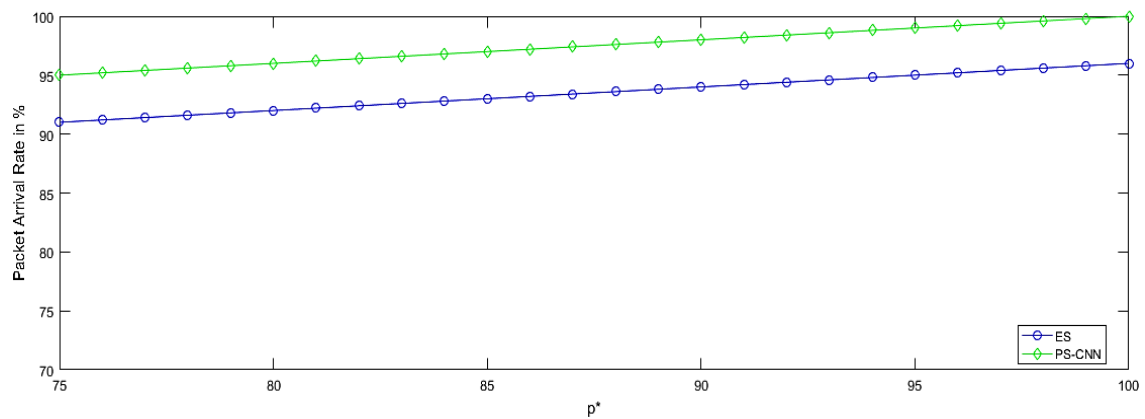


Figure 5. Comparison on PAR with existing algorithm at different parameters are  $W_1=0.1$  and  $W_2=0.5$

As seen in Figures 7 and 9, the amount of SNs and network energy are maximum for the proposed approach. The sample nodes have been optimized for existing algorithms to increase the network's performance to attain high PAR. As a result, the energy consumption of the network is increased. In any case, our CNN-based optimized BCAE algorithm uses less energy than the competition. Consumption could control the node energy inside a cluster because of the structure of energy. The nodes in a comparable cluster can communicate with one another when using the CNN-based optimized BCAE method. Additionally, other nodes don't need to transmit the sink node that can balance the network load.

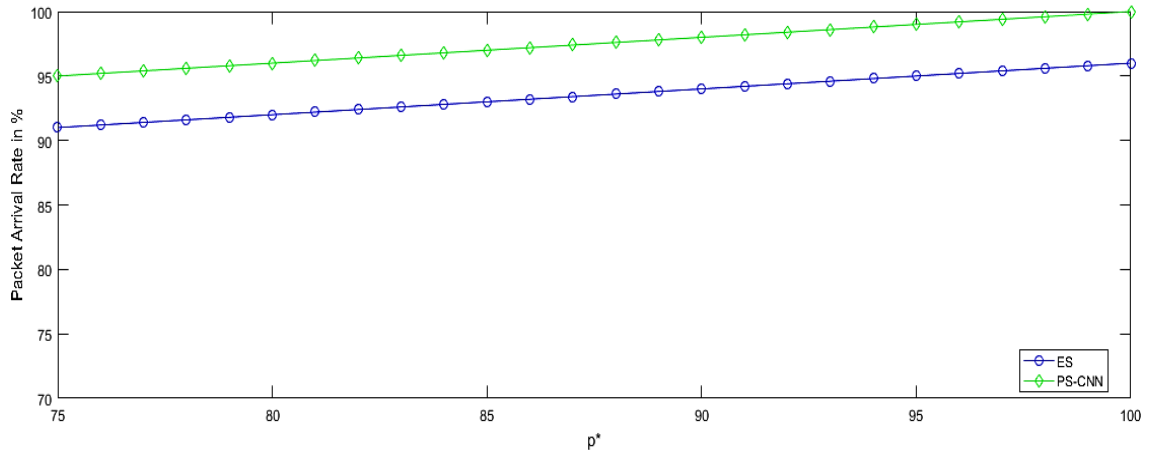


Figure 6. Comparison on PAR with existing algorithm at different parameters are  $W_1=0.4$  and  $W_2=0.9$

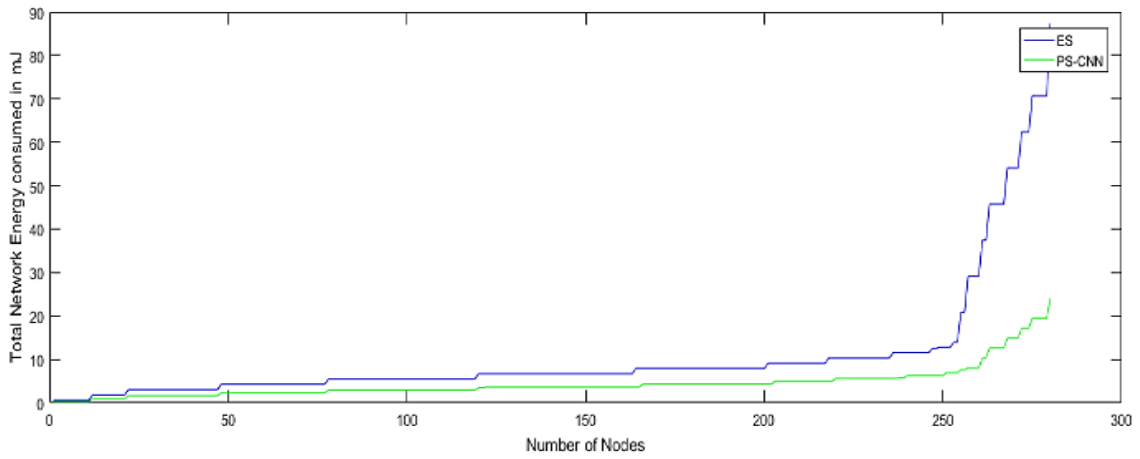


Figure 7. Comparison on energy consumption with existing algorithm at different parameters are  $W_1=0.5$  and  $W_2=0.9$

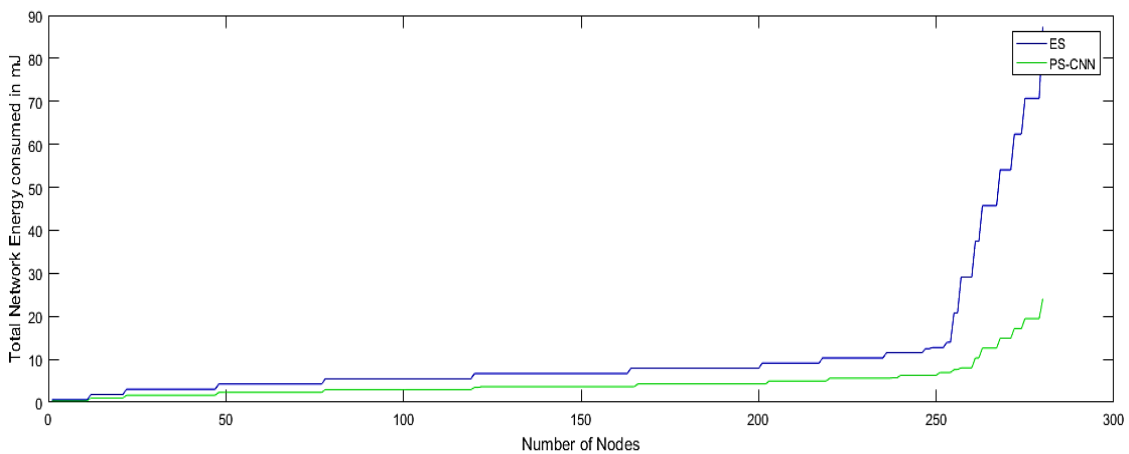


Figure 8. Comparison on energy consumption with existing algorithm at different parameters are  $W_1=0.1$  and  $W_2=0.5$

The transmission line's original signal and reconstructed signal are shown in Figures 10 to 12 with a training iteration count of 50. For evaluation 250 sample points are considered in the test set. The reconstructed signal may closely mirror the original signal's trend and value owing to the increased reconstruction precision provided by our proposed method. The black line in Figures 10 to 12 demonstrates that the original signal was successfully rebuilt using the reconstructed signal.

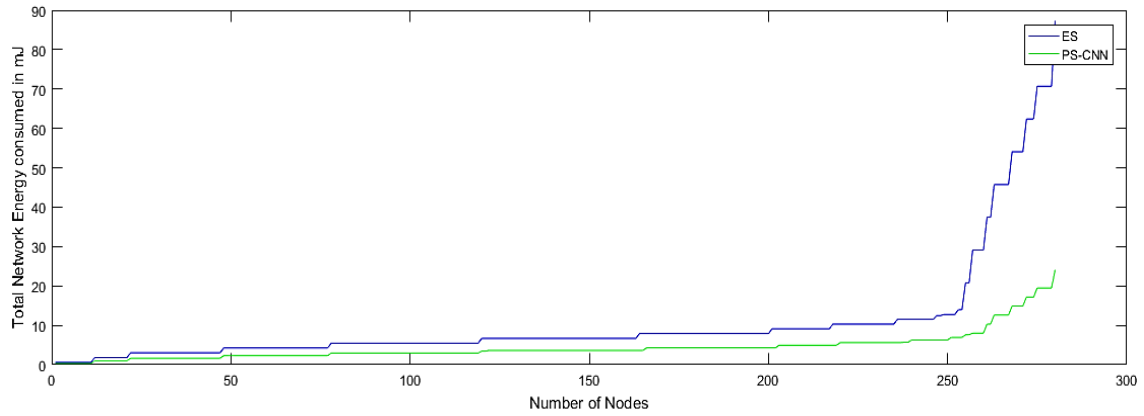


Figure 9. Comparison on network consumption with existing algorithm at different parameters are  $Ww_1=0.4$  and  $W_2=0.9$

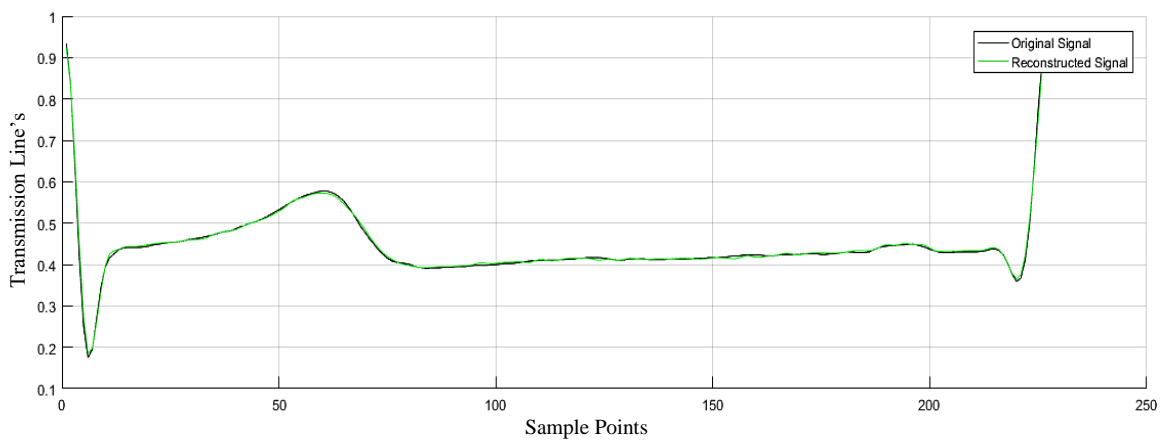


Figure 10. Original and reconstructed signal at various parameters  $W_1=0.5$  and  $W_2=0.9$

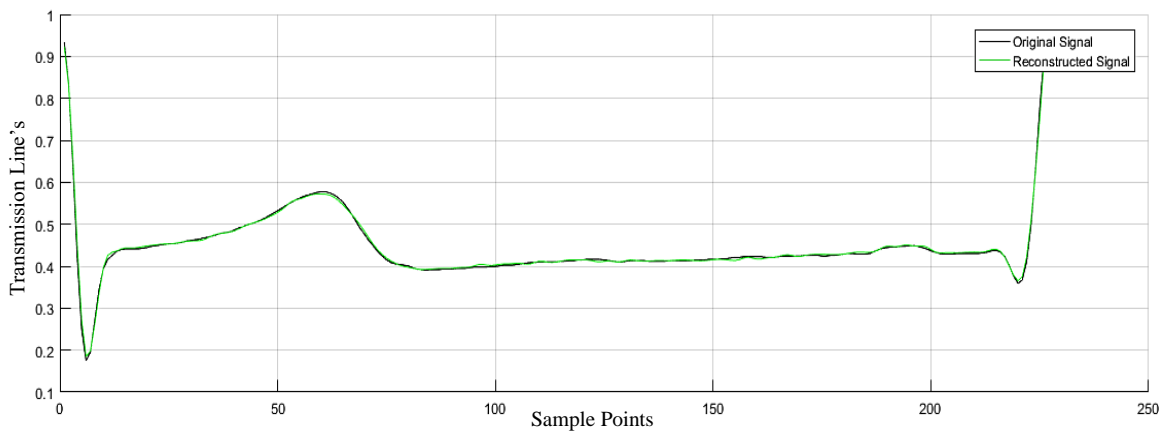


Figure 11. Original and reconstructed signal at various parameters  $W_1=0.1$  and  $W_2=0.5$

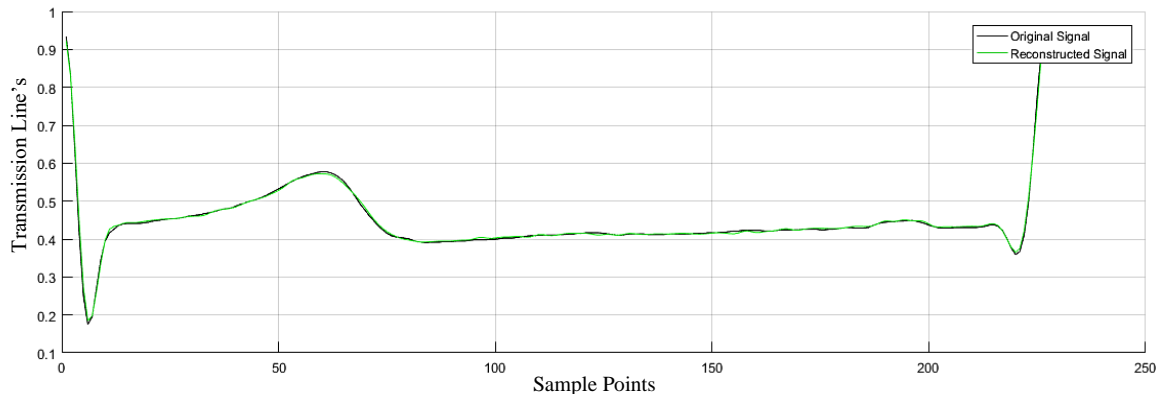


Figure 12. Original and reconstructed signal at various parameters  $W_1=0.4$  and  $W_2=0.9$

## 5. CONCLUSION

In this research, we proposed an efficient BCAC method based on CNN to integrate feature selection with auto-encoding for data transmission in the internet of things. We ran simulations on packet arrival rate, reconstruction, and energy usage to assess the efficacy of our suggested approach. It is demonstrated that the approach we suggested could provide precise reconstruction signals from the original signals. Additionally, this algorithm exhibits a great capacity for performance improvement. The primary improvement over the current technique is the precision of data reconstruction. Compared to current WSN algorithms, the suggested method may effectively reduce energy consumption for cluster nodes and network consumption, and increase network lifespan.




## REFERENCE

- [1] X. Liu and P. Zhang, "Data drainage: a novel load balancing strategy for wireless sensor networks," *IEEE Communications Letters*, vol. 22, no. 1, pp. 125–128, 2018, doi: 10.1109/LCOMM.2017.2751601.
- [2] X. Tang, H. Xie, W. Chen, J. Niu, and S. Wang, "Data aggregation based on overlapping rate of sensing area in wireless sensor networks," *Sensors (Switzerland)*, vol. 17, no. 7, 2017, doi: 10.3390/s17071527.
- [3] C. M. Sadler and M. Martonosi, "Data compression algorithms for energy-constrained devices in delay tolerant networks," in *SenSys'06: Proceedings of the Fourth International Conference on Embedded Networked Sensor Systems*, 2006, pp. 265–278, doi: 10.1145/1182807.1182834.
- [4] F. Marcelloni and M. Vecchio, "A simple algorithm for data compression in wireless sensor networks," *IEEE Communications Letters*, vol. 12, no. 6, pp. 411–413, 2008, doi: 10.1109/LCOMM.2008.080300.
- [5] D. I. Săcăleanu, R. Stoian, and D. M. Ofriim, "An adaptive Huffman algorithm for data compression in wireless sensor networks," in *ISSCS 2011-International Symposium on Signals, Circuits and Systems, Proceedings*, 2011, pp. 483–486, doi: 10.1109/ISSCS.2011.5978764.
- [6] Y. Chen, Q. Zhao, X. Hu, and B. Hu, "Multi-resolution parallel magnetic resonance image reconstruction in mobile computing-based IoT," *IEEE Access*, vol. 7, pp. 15623–15633, 2019, doi: 10.1109/ACCESS.2019.2894694.
- [7] Y. Liu, A. Liu, X. Liu, and X. Huang, "A statistical approach to participant selection in location-based social networks for offline event marketing," *Information Sciences*, vol. 480, pp. 90–108, 2019, doi: 10.1016/j.ins.2018.12.028.
- [8] V. Jelicic, M. Magno, D. Brunelli, V. Bilas, and L. Benini, "Benefits of wake-up radio in energy-efficient multimodal surveillance wireless sensor network," *IEEE Sensors Journal*, vol. 14, no. 9, pp. 3210–3220, 2014.
- [9] T. Mekonnen, P. Porambage, E. Harjula, and M. Ylianttila, "Energy consumption analysis of high quality multi-tier wireless multimedia sensor network," *IEEE Access*, vol. 5, pp. 15848–15858, 2017, doi: 10.1109/ACCESS.2017.2737078.
- [10] H. Jiang, S. Zhao, Z. Shen, W. Deng, P. A. Wilford, and R. Haimi-Cohen, "Surveillance video analysis using compressive sensing with low latency," *Bell Labs Technical Journal*, vol. 18, no. 4, pp. 63–74, 2014, doi: 10.1002/bltj.21646.
- [11] N. Y. Yu, K. Lee, and J. Choi, "Pilot signal design for compressive sensing based random access in machine-type communications," 2017, doi: 10.1109/WCNC.2017.7925686.
- [12] R. Mohammadian, A. Amini, and B. H. Khalaj, "Compressive sensing based pilot design for sparse channel estimation in OFDM systems," *IEEE communications letters*, vol. 21, no. 1, pp. 4–7, 2016.
- [13] S. K. Sharma, E. Lagunas, S. Chatzinotas, and B. Ottersten, "Application of compressive sensing in cognitive radio communications: A survey," *IEEE Communications Surveys and Tutorials*, vol. 18, no. 3, pp. 1838–1860, 2016, doi: 10.1109/COMST.2016.2524443.
- [14] M. A. Davenport, D. Takhar, J. N. Laska, T. Sun, K. F. Kelly, and R. G. Baraniuk, "Single-pixel imaging via compressive sampling," *IEEE Signal Processing Magazine*, pp. 83–91, 2008.
- [15] Q. Liang, "Compressive sensing for radar sensor networks," 2010, doi: 10.1109/GLOCOM.2010.5683674.
- [16] W. Ding *et al.*, "Spectrally efficient CSI acquisition for power line communications: a bayesian compressive sensing perspective," *IEEE Journal on Selected Areas in Communications*, vol. 34, no. 7, pp. 2022–2032, 2016, doi: 10.1109/JSAC.2016.2566140.
- [17] S. Qaisar, R. M. Bilal, W. Iqbal, M. Naureen, and S. Lee, "Compressive sensing: From theory to applications, a survey," *Journal of Communications and Networks*, vol. 15, no. 5, pp. 443–456, 2013, doi: 10.1109/JCN.2013.000083.
- [18] H. Huang, S. Misra, W. Tang, H. Barani, and H. Al-Azzawi, "Applications of compressed sensing in communications networks," *arXiv preprint arXiv:1305.3002*, 2013.




- [19] J. W. Choi, B. Shim, Y. Ding, B. Rao, and D. I. Kim, "Compressed sensing for wireless communications: useful tips and tricks," *IEEE Communications Surveys and Tutorials*, vol. 19, no. 3, pp. 1527–1550, 2017, doi: 10.1109/COMST.2017.2664421.
- [20] M. A. Razzaque, C. Bleakley, and S. Dobson, "Compression in wireless sensor networks: A survey and comparative evaluation," *ACM Transactions on Sensor Networks*, vol. 10, no. 1, 2013, doi: 10.1145/2528948.
- [21] H. A. Maw, H. Xiao, B. Christianson, and J. A. Malcolm, "BTG-AC: break-the-glass access control model for medical data in wireless sensor networks," *IEEE Journal of Biomedical and Health Informatics*, vol. 20, no. 3, pp. 763–774, 2016, doi: 10.1109/JBHI.2015.2510403.
- [22] E. M. Ar-Reyouchi, K. Ghoumid, D. Ar-Reyouchi, S. Rattal, R. Yahiaoui, and O. Elmazria, "Protocol wireless medical sensor networks in IoT for the efficiency of healthcare," *IEEE Internet of Things Journal*, vol. 9, no. 13, pp. 10693–10704, 2022, doi: 10.1109/JIOT.2021.3125886.
- [23] X. Yi, A. Bouguettaya, D. Georgakopoulos, A. Song, and J. Willemson, "Privacy protection for wireless medical sensor data," *IEEE Transactions on Dependable and Secure Computing*, vol. 13, no. 3, pp. 369–380, 2016, doi: 10.1109/TDSC.2015.2406699.
- [24] Y. K. Ever, "Secure-anonymous user authentication scheme for e-healthcare application using wireless medical sensor networks," *IEEE Systems Journal*, vol. 13, no. 1, pp. 456–467, 2019, doi: 10.1109/JSYST.2018.2866067.
- [25] X. Li, J. Peng, M. S. Obaidat, F. Wu, M. K. Khan, and C. Chen, "A secure three-factor user authentication protocol with forward secrecy for wireless medical sensor network systems," *IEEE Systems Journal*, vol. 14, no. 1, pp. 39–50, 2020, doi: 10.1109/JSYST.2019.2899580.
- [26] "Mimic II database," *PhysioNet*. <https://archive.physionet.org/mimic2/>.

## BIOGRAPHIES OF AUTHOR



**Usha Maniraju**    obtained her Bachelors of Engineering degree in CSE from VTU, Belagavi in 2007. She has obtained her master's degree in M. Tech (CSE) from VTU, Belagavi in 2013. Currently she is a research scholar at ACS College of Engineering, Bangalore pursuing her Ph.D. in Computer Science and Engineering and working as Assistant Professor at East West Institute of Technology. She has organized and attended many workshops and FDP's. Her areas of interest include internet of things, machine learning and cloud computing. She can be contacted at email: usharaj.@gmail.com.



**Thangamuthu Senthil Kumaran**    is a Dean and Professor at ACS College of Engineering, Department of Computer Science and Engineering Bangalore with an experience of 21 years in Teaching. He is qualified in Bachelor and Master Degrees in Computer Science and Engineering, and Ph.D. in Computer Science and Engineering in the area of data mining and big data. His areas of interest are wireless sensor networks, internet of things and big data analytics. He can be contacted at this email: senthilvts@gmail.com.